



UNIVERSITÀ DI PARMA

ARCHIVIO DELLA RICERCA

University of Parma Research Repository

Cone Calix[4]arenes with Orientable Glycosylthioureido Groups at the Upper Rim: An In-Depth Analysis of Their Symmetry Properties

This is the peer reviewed version of the following article:

Original

Cone Calix[4]arenes with Orientable Glycosylthioureido Groups at the Upper Rim: An In-Depth Analysis of Their Symmetry Properties / Legnani, Laura; Compostella, Federica; Sansone, Francesco; Toma, Lucio. - In: JOURNAL OF ORGANIC CHEMISTRY. - ISSN 0022-3263. - 80:15(2015), pp. 7412-7418. [10.1021/acs.joc.5b00878]

Availability:

This version is available at: 11381/2795972 since: 2021-10-05T13:45:59Z

Publisher:

American Chemical Society

Published

DOI:10.1021/acs.joc.5b00878

Terms of use:

Anyone can freely access the full text of works made available as "Open Access". Works made available

Publisher copyright

note finali coverpage

(Article begins on next page)

1 Cone Calix[4]arenes with Orientable Glycosylthioureido Groups at 2 the Upper Rim: An In-Depth Analysis of Their Symmetry Properties

3 Laura Legnani,[†] Federica Compostella,[‡] Francesco Sansone,[§] and Lucio Toma^{*,†}

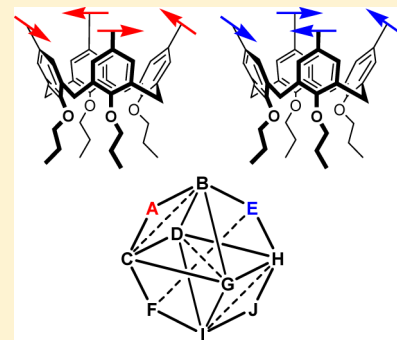
4 [†]Dipartimento di Chimica, Università di Pavia, Via Taramelli 12, 27100 Pavia, Italy

5 [‡]Dipartimento di Biotecnologie Mediche e Medicina Traslazionale, Università di Milano, Via Saldini 50, 20133 Milano, Italy

6 [§]Dipartimento di Chimica, Università di Parma, Parco Area delle Scienze 17/A, 43124 Parma, Italy

7 **S** Supporting Information

8 **ABSTRACT:** The two glycoclusters α - and β -D-mannosylthioureidocalix[4]arenes **1**
9 and **2** in the *cone* geometry have been submitted to a conformational investigation with
10 the DFT approach at the standard B3LYP/6-31G(d) level and using a water continuum
11 solvent model. After a reasoned choice of the level of calculation and the evaluation of
12 the properties of the monomeric components of **1** and **2**, the intrinsic conformational
13 properties of *cone* calix[4]arenes with orientable groups at the upper rim were
14 thoroughly analyzed. From the possible combinations of the directions that the groups
15 may assume, 10 different geometries derive, all chiral. These geometries are
16 interchangeable through two different processes, named breathing equilibrium and
17 arrow rotation, that allow a dense network connection among them. When the
18 modeling of whole macrocycles **1** and **2** was performed, a huge difference in their
19 conformational behavior that heavily influences the presentation mode of their
20 saccharidic moieties was found.



21 ■ INTRODUCTION

22 Multivalent presentation of carbohydrates using suitable
23 conjugation chemistry and scaffold selection may result in a
24 better efficiency and a higher selectivity in the interaction with
25 the corresponding receptors such as lectins and immunoglobulins.
26 The substituents linked to the scaffolds work as fingers
27 that may diverge from the central core or orient themselves
28 parallel to each other and converge toward one or more units of
29 a partner to interact with it. The nature of the scaffolds plays a
30 crucial role in the presentation of the substituents as well as the
31 nature of the linkers that connect to them. Calix[*n*]arenes, for
32 example, a well-known class of macrocycles, besides a series of
33 other applications,¹ have been successfully used as scaffolds for
34 multivalent presentation of saccharide moieties.^{2,3} The even-
35 numbered macrocycles ($n = 4, 6,$ and 8) have been mostly used.
36 The smallest member of this family of macrocycles ($n = 4$) has
37 the lowest mobility, and if the alkoxy groups at the lower rim
38 are large enough, stable conformational isomers that allow a
39 controlled display of the saccharide units in the space exist.
40 Several linkers with different flexibility have been exploited to
41 connect sugars to calixarenes.^{2,3} The more rigid ones can
42 heavily constrain the orientation options of the substituents so
43 that their presentation mode may be strongly affected.

44 In the literature, several glyco-calix[*n*]arenes in which glycosyl
45 moieties such as glucose, galactose, or lactose are linked as β
46 anomers, through a thiourea unit, to the upper rim of these
47 macrocyclic platforms have been reported.^{4–10} Despite of, or
48 perhaps because of, the proximity of the sugar epitopes to the
49 calixarene cavity, these glycosylthioureidocalixarenes have
50 shown in some cases very interesting inhibition properties

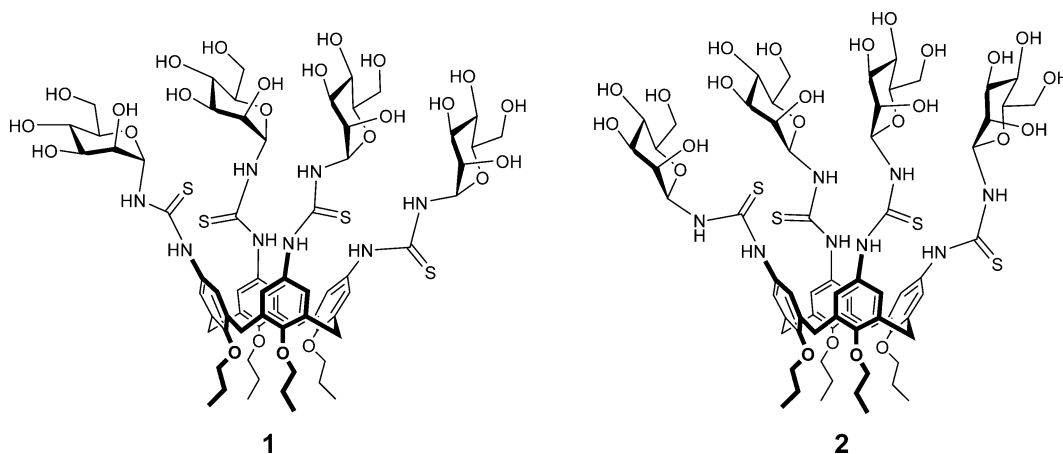
toward specific carbohydrate recognition proteins. Together 51
with a high efficiency often associated with a significant 52
multivalent effect, an impressive selectivity has been also 53
observed,⁴ for instance, in the binding of medically relevant 54
lectins, namely galectins, belonging to the same family. It is 55
interesting that the resulting selectivity strongly related to the 56
size and geometry of the glyco-calixarene. Tetralactosylcalix[4]-
57 arenes blocked in the *cone* geometry, i.e., that orienting the aryl
58 groups in the same direction, showed^{4,5} for example a strong
59 inhibition activity against galectin-3 and no activity against
60 galectin-1. 61

Another interesting point observed in the previous studies is 62
that a synthetic spacer like thiourea seems, at least in part, to 63
modify the natural specificity of the receptor for the substrate. 64
 β -Glucosylthioureidocalixarenes were in fact able to interact 65
with concanavalin A, a lectin known to be selective for natural 66
 α -manno- and α -glucosides.^{6,8} 67

On the basis of these data showing that glycosylthioureidocalixarenes 68
indeed make up an interesting class of selective 69
multivalent ligands, we focused on the *cone* calix[4]arene 70
scaffold and decided to investigate from a conformational point 71
of view the two glycoclusters **1** and **2**, both exposing mannosyl 72
moieties but differing in their anomeric configurations. Because 73
of the relevance of mannose in biology, these clusters could be 74
in the future synthesized and studied as inhibitors of lectins 75
involved in important processes. Actually, cluster **1**, where 76
mannose is present in the α -anomeric configuration, has 77

Received: April 20, 2015

Chart 1



78 recently been reported for the preparation of multivalent gold
79 nanoparticles.¹¹ On the other hand, to the best of our
80 knowledge, thioureidocalix[4]arene **2** containing β -mannosyl
81 moieties has never been synthesized. In a sort of predictive
82 challenge, in this investigation the two potential multivalent
83 ligands have been compared to gain insight into the effects of
84 the anomeric configuration of the sugar on the presentation
85 mode of the saccharide portion of glyoclusters.

86 Thus, we have undertaken an in-depth theoretical study of α -
87 and β -D-mannosylthioureidocalix[4]arenes **1** and **2** (Chart 1),
88 and following our usual approach to dissecting the problem in
89 all its components, we have faced step by step the several
90 computational items involved in the study: the choice of the
91 suitable level of calculation, the evaluation of the properties of
92 each monomeric component of calixarenes **1** and **2**, the need to
93 deepen our knowledge of the intrinsic conformational proper-
94 ties of *cone* calix[4]arenes with orientable groups at the upper
95 rim, and, just at the end, modeling whole macrocycles **1** and **2**,
96 including their chiral mannosyl moieties.

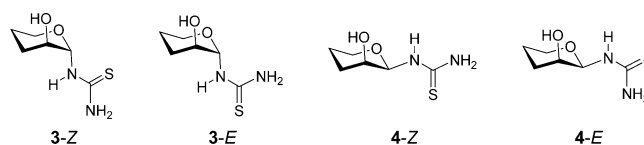
97 ■ RESULTS AND DISCUSSION

98 **Choice of the Computational Method.** In a modeling
99 study, the choice of the computational approach is of utmost
100 importance for a correct description of the system. In the
101 framework of the widely used density functional theory,
102 attention was focused on the standard B3LYP/6-31G(d)
103 level^{12,13} as the large molecular size of **1** and **2** did not allow
104 the use of higher theory levels, which would cause unreasonably
105 longer computational time. The first goal was to verify the
106 suitability of this approach in correctly describing the different
107 functionalities in the molecules, i.e., the thioureido group and
108 the glycosides. In the thioureido units, the restricted rotation of
109 the pseudoamide NH-C=S bonds and the consequent
110 tendency to planarity allow the existence of the four
111 geometrical isomers designated as ZZ, ZE, EZ, and EE. An
112 extensive MP2/aug-cc-pVDZ study¹⁴ of alkyl- and phenyl-
113 substituted thiourea derivatives showed that conformations
114 with alkyl groups *Z* to the sulfur atom are more stable by 0.4–
115 1.5 kcal/mol than the *E* forms. In contrast, analysis of
116 phenylthiourea revealed that in this case the opposite *E* isomer
117 is preferred by 2.65 kcal/mol.

118 In compounds **1** and **2**, the substituents at the two sides of
119 thiourea are a *p*-propoxyphenyl and a glycan. In analogy with
120 the MP2 data for phenylthiourea mentioned above, a
121 propoxyphenylthiourea should present a clear preference for

the *E* geometry. To the best of our knowledge, no calculations
122 at the MP2 level of theory have been performed on
123 glycosylthioureas, so that their conformational preferences
124 have to be investigated. Therefore, we decided to model at this
125 level the simplified structures **3** and **4** (Chart 2). They present a
126 c2

Chart 2



thiourea at the anomeric position in the α or β orientation and
127 an axially oriented hydroxyl group at position 2 of a pyranose
128 ring in the ⁴C₁ conformation, respectively, maintaining the main
129 structural features required for a correct description of the
130 mannosyl–thiourea interaction.
131

The *E* and *Z* geometries of compounds **3** and **4** were built
132 and optimized at the MP2/aug-cc-pVDZ level. Table 1 reports
133 t1

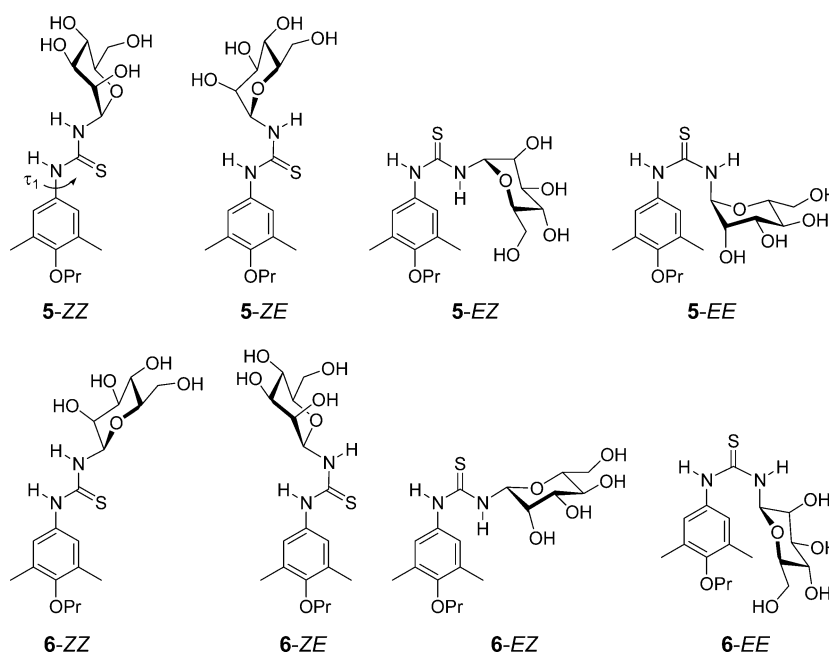
Table 1. Relative Energies (kilocalories per mole) of the *E* and *Z* Geometries of Compounds **3 and **4** Optimized at Different Levels of Theory**

	MP2/aug-cc-pVDZ	B3LYP/6-31G(d)	B3LYP/6-31G(d) ^a
<i>E</i> -3	0.00	0.00	0.00
<i>Z</i> -3	6.35	7.23	3.42
<i>E</i> -4	0.00	0.00	0.00
<i>Z</i> -4	1.53	2.30	1.57
<i>E</i> -phenylthiourea	0.00 ^b	0.00	0.00
<i>Z</i> -phenylthiourea	2.65 ^b	3.92	2.54

^aOptimization performed in a polarizable continuum solvent model (PCM) choosing water as the solvent. ^bData from ref 14.

the relative energies of the optimized structures. In both cases,
134 the *E* geometry is preferred over the *Z* one. Then we tested the
135 DFT B3LYP functional, using the 6-31G(d) basis set, for its
136 ability to reproduce the MP2 stability data; thus, we optimized
137 in vacuum, at this level of theory, a couple of *E*/*Z* isomers of
138 thioureas **3** and **4** as well as phenylthiourea (Table 1). The
139 DFT approach was able to reproduce the greater stability of the
140 *E* isomer of the three computed N-substituted thioureas with
141 an energy difference even greater than that computed at the
142

Chart 3



143 MP2 level. Moreover, considering that vacuum optimization on
 144 saccharide compounds might be biased by the excessive
 145 strength of the hydrogen bonds involving the hydroxyl groups,
 146 the structures were optimized again taking into consideration
 147 the solvent effect by using a polarizable continuum model
 148 (PCM)^{15–17} and choosing water as the solvent. Once more, the
 149 *E* isomers were more stable, though the values of the relative
 150 energy of the *Z* isomers were smaller than in the in vacuum
 151 optimizations. It is worth pointing out that the DFT approach
 152 combined with the solvent effect gives results comparable with
 153 those obtained with the MP2 approach over a much shorter
 154 computational time. Thus, throughout this work, all calcu-
 155 lations were performed at the B3LYP/6-31G(d) level through
 156 optimizations in the PCM solvent model of water.

157 **Modeling of Monomers 5 and 6.** In a stepwise approach
 158 to the study of the entire calixarenes, the conformational
 159 behavior of the single model monomeric α - and β -D-
 160 mannopyranosylthioureas **5** and **6** (Chart 3) was investigated and
 161 the results are reported in Table 2. The aryl and glycosyl groups

the *EE* arrangement becomes the least stable one. Therefore, 169
 structures having one NH=C=S bond in the *E* geometry and 170
 the other in the *Z* geometry are found to be the global minima 171
 for both **5** and **6**, with the *ZE* geometry preferred by **5** and the 172
EZ geometry by its β -anomer **6** (Table 2). This different 173
 behavior is a consequence of the relative stability of the *E* and *Z* 174
 isomers reported in Table 1, where it is shown that the *E* – *Z* 175
 energy difference for **3** is larger than for phenylthiourea, which 176
 is the opposite of the case for **4**, which shows a smaller *E* – *Z* 177
 energy difference. The *ZZ* geometry was found to be less stable 178
 than the global minimum by ~ 3 kcal/mol in both compounds. 179

The three-dimensional plots reported in Figure 1 show that 180 f
 the *ZZ* and *ZE* geometries determine an almost extended shape 181
 for the molecules that, on the contrary, assume a bent shape in 182
 the *EZ* and *EE* geometries; in the latter cases, the steric strain 183
 between the sugar and the phenyl ring is released by deviation 184
 of thiourea from planarity. Moreover, because of conjugation, 185
 there is the tendency of thiourea and phenyl to coplanarity; this 186
 tendency is hindered by the interactions of the phenyl *meta* 187
 hydrogens with the NH hydrogen or the CS sulfur atoms that 188
 lead to a plane between the two groups of approximately 50– 189
 60°. Thus, for each thiourea geometry, there are two possible 190
 orientations with respect to phenyl that are not isoenergetic, 191
 because of the chirality of the monosaccharide. They are 192
 distinguished by the descriptors *a* and *b* in Table 2 and Figure 193
 1, assigned on the basis of the dihedral angle τ_1 , defined by the 194
 atoms C3–C4–N–C(=S) (Chart 3), with *a* used for $90^\circ < \tau_1$ 195
 $< 270^\circ$ and *b* for $-90^\circ < \tau_1 < 90^\circ$. 196

Symmetry Properties of cone-Calix[4]arenes Substituted at the Upper Rim. When four propoxy groups are 197
 present at the lower rim of calix[4]arenes, as in the case of **1** 198
 and **2**, the macrocycle is locked in specific conformations, 199
 named by Gutsche¹⁸ as *cone*, *partial cone*, 1,3-alternate, and 1,2- 201
 alternate, differing for the orientation of the phenyl groups. In 202
 the *cone* conformation, the four aryl groups are oriented in the 203
 same direction, the origin of a geometry usually represented as 204
 a C_4 symmetrical structure. However, the minimum energy 205
 geometry is better described as a C_2 symmetrical structure, the 206

Table 2. Relative Energies (kilocalories per mole) of the Four Geometrical Isomers of Compounds 5 and 6 Optimized at the B3LYP/6-31G(d) Level in a Water Continuum Solvent Model

	<i>ZZ-a</i>	<i>ZE-a</i>	<i>EZ-a</i>	<i>EE-a</i>	<i>ZZ-b</i>	<i>ZE-b</i>	<i>EZ-b</i>	<i>EE-b</i>
5	3.48	0.00	0.56	7.31	3.48	0.80	0.66	4.77
6	2.84	<i>a</i>	0.00	4.36	2.84	0.95	0.02	4.98

^aMinimum not located. It converges to the *ZE-b* conformer during the optimization.

162 on the two sides of thiourea should have, as discussed above, a
 163 defined preference for the *E* geometry at the respective
 164 pseudoamide NH=C=S bond. Indeed, the *EE* geometry suffers
 165 from a severe steric strain involving the aryl and sugar moieties
 166 that is in part released through a deviation from planarity of the
 167 thioureido group, leading to stereoelectronic destabilization.
 168 Despite this balance between steric and stereoelectronic factors,

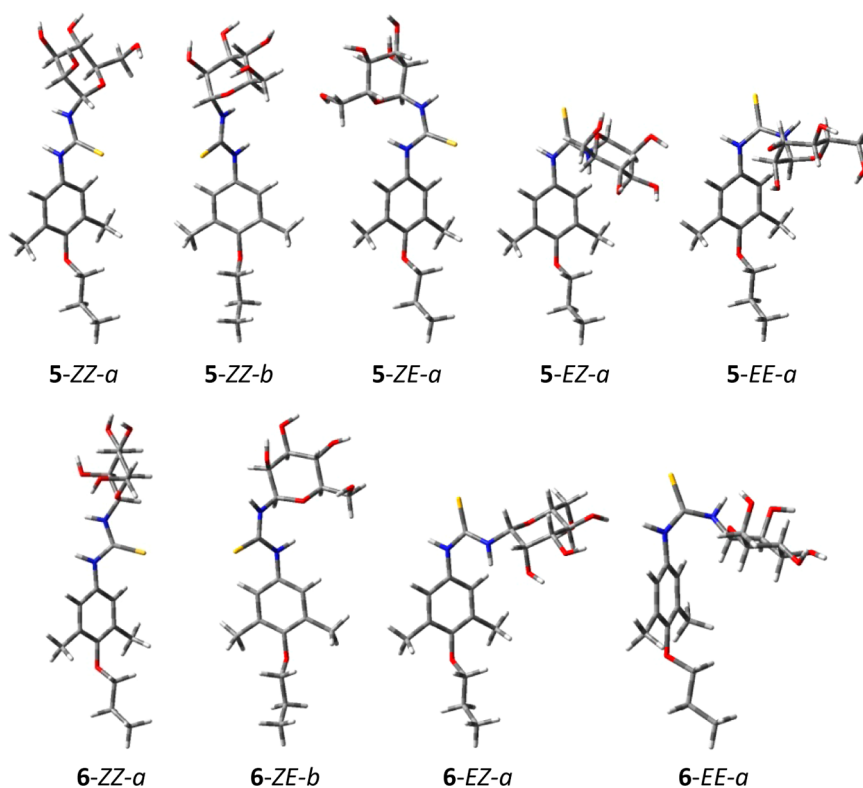


Figure 1. Three-dimensional plot of the ZZ, ZE, EZ, and EE conformers of monomeric α - and β -D-mannosylthioureas 5 and 6.

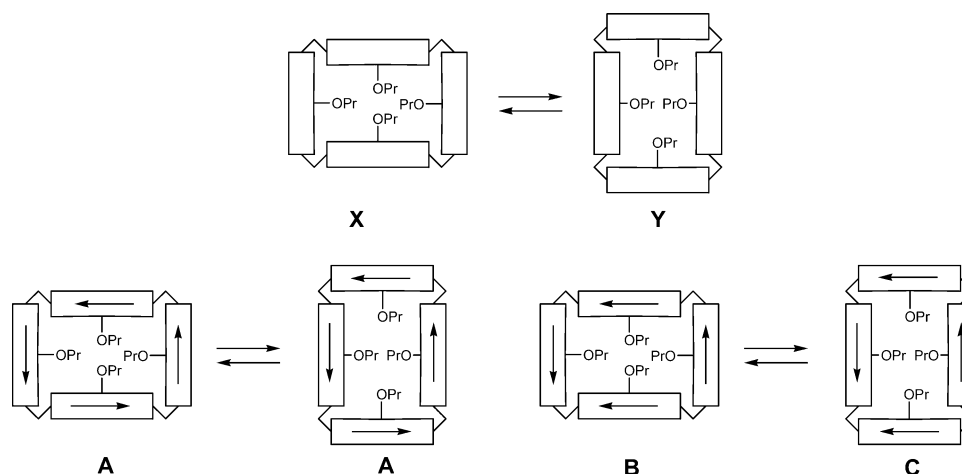


Figure 2. Schematic representation of the breathing equilibrium of *cone*-calix[4]arenes without (X and Y) and with (A–C) orientable groups at the upper rim.

207 so-called *pinched cone* conformation, that has two opposite
 208 phenyl groups at a distance much shorter than that between the
 209 other two. However, an easy equilibrium, in which the farther
 210 groups have approached and the closer ones have moved away,
 211 interchanges the close and far phenyl groups, making them
 212 indistinguishable.¹⁹ This equilibrium between the *pinched cone*
 213 conformations, which could be called the breathing equilibrium,
 214 can be schematically represented using rectangular-shaped
 215 drawings in which the macrocycle is seen from a top view
 216 (Figure 2, X \rightleftharpoons Y equilibrium).

217 The X and Y structures are indistinguishable, but when at the
 218 upper rim of calixarene are introduced groups that may assume
 219 two different orientations with respect to the phenyl rings, as
 220 for example the thiourea groups, a series of distinguishable

conformers can exist. In Figure 2, the orientable groups are 221
 represented as arrows that can be arranged in combinations 222
 such as those indicated as A–C in Figure 2. The breathing 223
 equilibrium on these structures may produce a conformer 224
 indistinguishable from the starting one, as in the case of A, or a 225
 distinct conformer, as in the B \rightleftharpoons C equilibrium. A total of 10 226
 different combinations do exist; these 10 conformers, A–J, are 227
 drawn in a simpler, more schematic, way in Figure 3. The 228
 conformers can interconvert through the breathing equilibrium 229
 (B/C, D/G, E/F, and H/I) or through the rotation of an 230
 orientable group (arrow) with respect to the phenyl group to 231
 which it is linked. For example, A can be converted into B or C 232
 through the rotation of just one arrow; in turn, B can be 233
 converted into D, E, or G, etc. These transformations can be 234

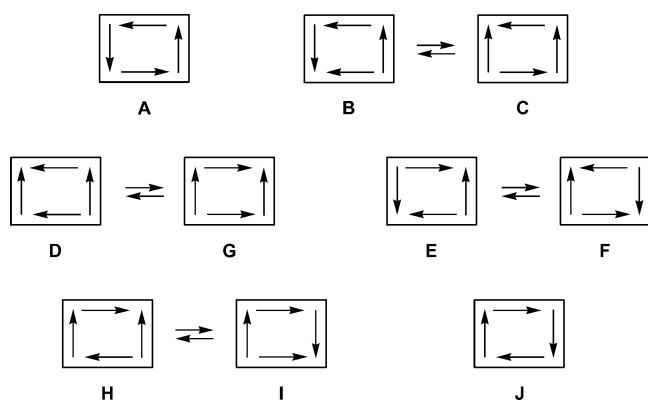


Figure 3. Schematic representation of the 10 conformations (A–J) of a cone-calix[4]arene with four orientable groups at the upper rim.

minimum conformers of compound **5**, by selecting the *ZE* 265 geometry for the thiourea and considering that the *ZE-a* and 266 *ZE-b* geometries correspond to the right- and left-oriented 267 arrows, respectively, in the schematic representations in Figure 268 **3** when observed from a point of view external to the calix core. 269 First, a geometry of A type was built, i.e., *ZE-a* geometries for 270 the orientation of the four thiourea groups. It was optimized at 271 the same calculation level used for the monomers, yielding the 272 **1A-ZE** conformer reported in Figure 5. 273

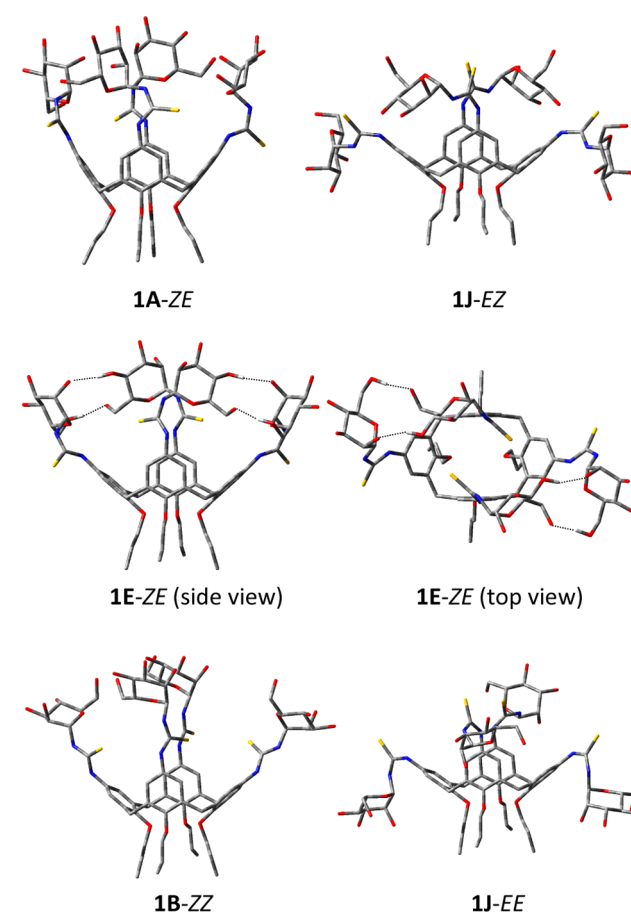


Figure 5. Three-dimensional plots of conformers **1A-ZE**, **1E-ZE**, **1J-EZ**, **1B-ZZ**, and **1J-EE** of α -D-mannosylthioureidocalix[4]arene **1**. The hydrogen atoms have been omitted for the sake of clarity except those involved in the inter-residue H-bonds of **1E-ZE**.

From this conformer, nine new starting geometries were built 274 up, through suitable rotations of the thiourea groups with 275 respect to the corresponding phenyl group (arrow rotations), 276 and optimized. The relative energies of all 10 minimum energy 277 conformers so obtained are reported in Table 1S (Supporting 278 Information) together with the percentage populations at 298 279 K calculated with the Boltzmann equation. The global 280 minimum, conformer **1E-ZE**, was largely preferred. In fact, 281 the second and third conformers, **1C-ZE** and **1A-ZE**, 282 respectively, were less stable by 3.09 and 4.43 kcal/mol, 283 respectively, so that **1E-ZE** accounts for more than 99% of the 284 overall population. Its three-dimensional plot is reported in 285 Figure 5, whereas those of the other conformers are reported in 286 Figure 1S (Supporting Information). Conformer **1E-ZE** has a 287 C_2 symmetrical geometry with adjacent couples of mannosyl 288 residues interacting through hydrogen bonds. It is noteworthy 289

235 represented by a graph (Figure 4) in which each solid line 236 connects conformers that can be interchanged through rotation

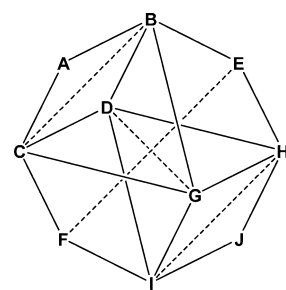


Figure 4. Graph representing the connections among the 10 A–J conformations of a cone-calix[4]arene with four orientable groups at the upper rim through arrow rotations (solid lines) or breathing equilibria (dashed lines).

237 of an arrow and the dashed lines connect conformers that can 238 be interchanged through the breathing equilibrium. At the two 239 extremes are the counterclockwise (**A**) and clockwise (**J**) arrow 240 arrangements that obviously require four arrow rotations to be 241 converted one into the other.

242 All of the A–J geometries are chiral. Moreover, they can be 243 grouped into five enantiomeric pairs, **A** and **J**, **B** and **I**, **C** and **H**, 244 **D** and **G**, and **E** and **F**; i.e., all the pairs at the opposite vertices 245 of the graph of Figure 4 are enantiomerically related and hence 246 isoenergetic. When the orientable groups contain chiral 247 elements, all of the A–J geometries become diastereoisomeric 248 so that each of them presents a different energy value.

249 **Modeling of Calixarenes 1 and 2.** The complete 250 structures of α - and β -D-mannosylthioureidocalix[4]arenes (**1** 251 and **2**) were then built on the basis of the optimized 252 monomeric structures **5** and **6** and taking into account the 253 symmetry properties of cone calixarenes with orientable groups 254 at the upper rim discussed above. The complete exploration of 255 the conformational space of **1** and **2** through a systematic 256 search approach may become very demanding. However, we 257 decided to use this approach, instead of a molecular dynamics 258 approach based on an empirical force field method, to 259 guarantee an appropriate description of the different function- 260 alities present in the molecules, in particular the thiourea 261 groups. The procedure first exemplified for **1** was successively 262 applied to compound **2**.

263 Thus, we built starting geometries for α -D- 264 mannosylthioureidocalix[4]arene **1** based on the energy

290 that the four mannosyl residues are not equivalent, each couple
291 being identical at the opposite sides of the molecule; in fact,
292 two residues expose their β -face outward and the other two
293 their α -face. As shown in the graph in Figure 4, to interchange
294 these two residues, at least one breathing equilibrium and four
295 arrow rotations are necessary, passing through four conformers
296 with energies higher than that of **1E-ZE** (Scheme 1S,
297 Supporting Information). Therefore, the interchange of the
298 two couples of residues should be rather difficult as a series of
299 arrow rotations are necessary; moreover, these are much more
300 difficult in **1E-ZE** than in monomer **5** as they require the
301 breaking of the network of inter-residue hydrogen bonds.

302 Though the *ZE* orientation of the thiourea is preferred in
303 monomer **5**, it is necessary to ascertain that this conformational
304 preference is maintained in **1**. Thus, the procedure described
305 above for the *ZE* geometry was repeated for the three other
306 thiourea geometries optimizing in each case the 10
307 corresponding **A–J** conformations; the data of the preferred
308 conformer for each thiourea geometry, **1J-EZ**, **1B-ZZ**, and **1J-**
309 **EE**, are reported in Table 1S (Supporting Information). All
310 these geometries were shown to be much less stable than **1E-**
311 **ZE**, their relative energies being 9.19, 12.06, and 33.00 kcal/
312 mol, respectively. Their three-dimensional plots are reported in
313 Figure 5.

314 The approach used for the modeling of compound **1** was
315 then applied to β -D-mannosylthioureidocalix[4]arene **2**, and the
316 results are summarized in Table 2S and Figure 2S (Supporting
317 Information). In this case, a definite preference for the *EZ*
318 geometry of the thiourea group was found and the global
319 minimum conformer, accounting for almost 90% of the overall
320 population, was shown to be **2A-EZ** (Figure 6), with the

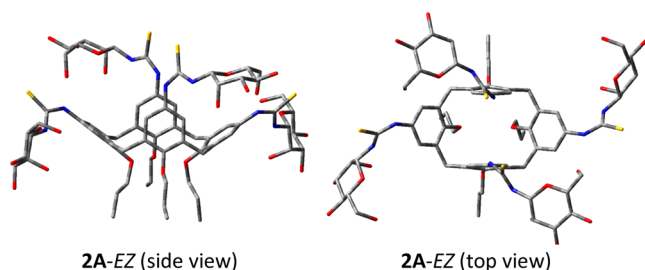


Figure 6. Three-dimensional plots of the global minimum conformer **2A-EZ** of β -D-mannosylthioureidocalix[4]arene **2**. The hydrogen atoms have been omitted for the sake of clarity.

321 remaining 10% attributable to its **2G-EZ**, **2B-EZ**, and **2E-EZ**
322 graph neighbors. The other thiourea geometries were shown to
323 be less stable; in fact, the corresponding preferred **2I-ZE**, **2I-ZZ**,
324 and **2A-EE** conformers showed relative energy values of 5.67,
325 8.84, and 25.56 kcal/mol, respectively. As for calixarene **1**, the
326 global minimum conformer of calixarene **2**, **2A-EZ**, has a C_2
327 symmetrical geometry with two couples of identical opposite β -
328 mannosyl residues. However, it should be noted that in
329 conformer **2A-EZ** these residues point outward with respect to
330 the calix core so that no inter-residue hydrogen bond can be
331 established. This allows a certain degree of conformational
332 mobility that makes the arrow rotations easier than in the case
333 of the α -anomer.²⁰ Moreover, the two couples of sugar residues
334 can easily interconvert; in fact, the breathing equilibrium from
335 **2A-EZ** yields an identical **A**-type geometry with interchanged
336 mannose residues (Scheme 2S, Supporting Information), thus
337 making the four sugar residues actually indistinguishable.²¹

CONCLUSIONS

338

339 With the final goal of investigating the conformational
340 properties of two α - and β -mannosyl glycoclusters, and
341 highlighting their similarities and differences, we had to deal
342 with the problem of the multiple arrangements allowed to *cone*
343 calix[4]arenes functionalized with orientable groups at the
344 upper rim. A systematic analysis of the possible orientations of
345 these groups evidenced specific symmetry properties that can
346 heavily influence the overall conformational behavior.

347 A restricted rotation around the bond connecting the phenyl
348 groups of calixarenes to the functionality at their 4 position
349 allows the definition of the substituent as an orientable group
350 when this functionality is nonsymmetric in its nature. The
351 presence of orientable groups at the upper rim gives rise to 10
352 different geometries schematically represented as **A–J** in Figure
353 3. These geometries are chiral structures corresponding to five
354 enantiomeric pairs. Their interconversion relies onto two
355 different processes, the breathing equilibrium and the arrow
356 rotation. Depending on the extent of conjugation of the
357 orientable group with the phenyl and the possibility of the
358 groups linked to the calixarene structure establishing through-
359 space interaction such as hydrogen bonds, the 10 geometries
360 (**A–J**) are more or less easily interconvertible.

361 The theoretical study of α - and β -D-mannosylthioureidocalix-
362 [4]arenes **1** and **2** evidenced a huge difference in their
363 conformational behavior that heavily influences the presenta-
364 tion mode of the saccharidic moieties. The preference of **1** for
365 the *ZE* geometry of thiourea determines an extended shape of
366 each monomeric unit. This allows the formation of hydrogen
367 bonds between adjacent couples of mannosyl residues. The
368 optimal orientation of these residues corresponds to that
369 defined by the *E*-type geometry in which hydrogen bonds are
370 established among the hydroxyl groups at positions 4 and 6 of
371 one residue and those at positions 6 and 2 of the other.
372 Moreover, the residues expose alternatively their α or β face
373 outward, and consequently, the four mannosyl residues are not
374 equivalent. The β -isomer **2**, conversely, shows a neat preference
375 for the *EZ* geometry of thiourea with a bent shape that turns
376 the mannosyl residues away from the calixarene core preventing
377 the formation of any inter-residue hydrogen bond. Con-
378 sequently, **2** prefers the **A**-type geometry in which the four
379 mannosyl residues can easily be interchanged simply through a
380 breathing equilibrium between two *pinched cone* conformers.

381 In conclusion, though the two isomeric glycoclusters differ
382 only in the anomeric configuration of the sugar, a great
383 difference in their overall geometry has been evidenced so that
384 a very different ability to interact with a protein partner can be
385 hypothesized, in a manner independent of the native selectivity
386 of the receptor observed for one anomer or the other in natural
387 substrates. This shows that the preliminary knowledge of the
388 conformational properties of a calixarene glycocluster can
389 become a powerful tool in driving the synthetic work toward
390 the targets that are predicted to better fit the desired features
391 for a useful multivalent presentation.

COMPUTATIONAL METHODS

392

393 All the calculations were conducted using the Gaussian09 program
394 package.²² All the structures were optimized at the B3LYP/6-31G(d)
395 level^{12,13} in the water solvent simulated using a self-consistent reaction
396 field (SCRF) method, based on a polarizable continuum solvent model
397 (PCM).^{15–17}

398 ■ ASSOCIATED CONTENT

399 ■ Supporting Information

400 Schemes 1S and 2S, Tables 1S and 2S, Figures 1S and 2S, and
401 electronic energy and Cartesian coordinates of all computed
402 structures. The Supporting Information is available free of
403 charge on the ACS Publications website at DOI: 10.1021/
404 acs.joc.5b00878.

405 ■ AUTHOR INFORMATION

406 Corresponding Author

407 *E-mail: lucio.toma@unipv.it. Telephone: (+39) 0382987843.
408 Fax: (+39) 0382987323.

409 Notes

410 The authors declare no competing financial interest.

411 ■ ACKNOWLEDGMENTS

412 The Italian Ministry of University and Research (Grant PRIN
413 2010-11, prot. 2010JMAZML, Italian network for the develop-
414 ment of multivalent nanosystems) is gratefully acknowledged
415 for financial support. CINECA is also acknowledged for the
416 allocation of computer time.

417 ■ REFERENCES

- 418 (1) Sansone, F.; Baldini, L.; Casnati, A.; Ungaro, R. *New J. Chem.*
419 **2010**, *34*, 2715–2728.
- 420 (2) Sansone, F.; Casnati, A. *Chem. Soc. Rev.* **2013**, *42*, 4623–4639.
- 421 (3) Dondoni, A.; Marra, A. *Chem. Rev.* **2010**, *110*, 4949–4977.
- 422 (4) André, S.; Sansone, F.; Kaltner, H.; Casnati, A.; Kopitz, J.; Gabius,
423 H.-J.; Ungaro, R. *ChemBioChem* **2008**, *9*, 1649–1661.
- 424 (5) André, S.; Grandjean, C.; Gautier, F.-M.; Bernardi, S.; Sansone,
425 F.; Gabius, H.-J.; Ungaro, R. *Chem. Commun.* **2011**, *47*, 6126–6128.
- 426 (6) Sansone, F.; Chierici, E.; Casnati, A.; Ungaro, R. *Org. Biomol.*
427 *Chem.* **2003**, *1*, 1802–1809.
- 428 (7) Torvinen, M.; Neitola, R.; Sansone, F.; Baldini, L.; Ungaro, R.;
429 Casnati, A.; Vainiotalo, P.; Kalenius, E. *Org. Biomol. Chem.* **2010**, *8*,
430 906–915.
- 431 (8) Sansone, F.; Baldini, L.; Casnati, A.; Ungaro, R. *Supramol. Chem.*
432 **2008**, *20*, 161–168.
- 433 (9) Consoli, G. M. L.; Cunsolo, F.; Geraci, C.; Mecca, T.; Neri, P.
434 *Tetrahedron Lett.* **2003**, *44*, 7467–7470.
- 435 (10) Consoli, G. M. L.; Cunsolo, F.; Geraci, C.; Sgarlata, V. *Org. Lett.*
436 **2004**, *6*, 4163–4166.
- 437 (11) Avvakumova, S.; Fezzardi, P.; Pandolfi, L.; Colombo, M.;
438 Sansone, F.; Casnati, A.; Prospero, D. *Chem. Commun.* **2014**, *50*,
439 11029–11032.
- 440 (12) Becke, A. D. *J. Chem. Phys.* **1993**, *98*, 5648–5652.
- 441 (13) Lee, C.; Yang, W.; Parr, R. G. *Phys. Rev. B: Condens. Matter*
442 *Mater. Phys.* **1988**, *37*, 785–789.
- 443 (14) Bryantsev, V. S.; Hay, B. P. *J. Phys. Chem. A* **2006**, *110*, 4678–
444 4688.
- 445 (15) Cancés, E.; Mennucci, B.; Tomasi, J. *J. Chem. Phys.* **1997**, *107*,
446 3032–3042.
- 447 (16) Cossi, M.; Barone, V.; Cammi, R.; Tomasi, J. *Chem. Phys. Lett.*
448 **1996**, *255*, 327–335.
- 449 (17) Barone, V.; Cossi, M.; Tomasi, J. *J. Comput. Chem.* **1998**, *19*,
450 404–417.
- 451 (18) Stoddart, J. F. *Calixarenes: An Introduction*; Gutsche, C. D., Ed.;
452 The Royal Society of Chemistry: Cambridge, U.K., 2008; p 276.
- 453 (19) Arduini, A.; Fabbri, M.; Mantovani, M.; Mirone, L.; Pochini, A.;
454 Secchi, A.; Ungaro, R. *J. Org. Chem.* **1995**, *60*, 1454–1457.
- 455 (20) As the molecular size of these mannosylthioureidocalix[4]arenes
456 is too large to allow the location of the transition state corresponding
457 to the arrow rotation at the chosen computational level, including the
458 continuum solvent model, the energy barriers for the conversion of
459 1E-ZE to its graph neighbor 1B-ZE, as well as that between 2A-EZ and
460 2B-EZ, were estimated through a relaxed potential energy surface scan

of the proper dihedral angle τ_1 . The former barrier was shown to be
461 13–14 kcal/mol, whereas the latter was only ~ 5 kcal/mol, thus
462 indicating that the arrow rotation is much easier in **2** than in **1**.

(21) To estimate the energy barrier relative to the breathing
463 equilibrium, a simplified structure, obtained from **2A-EZ** by deleting
464 the four saccharide moieties, was optimized. It is expected that this
465 simplification does not significantly alter the barrier value, as the sugars
466 point outward with respect to the calix core. The corresponding
467 transition state was also built and optimized both in vacuo and in
468 water. Calculations showed an energy barrier of 7.81 kcal/mol that
469 becomes even lower (6.14 kcal/mol) with solvation, thus highlighting
470 the easiness of this interconversion.

(22) Frisch, M. J.; Trucks, G. W.; Schlegel, H. B.; Scuseria, G. E.;
471 Robb, M. A.; Cheeseman, J. R.; Scalmani, G.; Barone, V.; Mennucci,
472 B.; Petersson, G. A.; Nakatsuji, H.; Caricato, M.; Li, X.; Hratchian, H.
473 P.; Izmaylov, A. F.; Bloino, J.; Zheng, G.; Sonnenberg, J. L.; Hada, M.;
474 Ehara, M.; Toyota, K.; Fukuda, R.; Hasegawa, J.; Ishida, M.; Nakajima,
475 T.; Honda, Y.; Kitao, O.; Nakai, H.; Vreven, T.; Montgomery, J. A., Jr.;
476 Peralta, J. E.; Ogliaro, F.; Bearpark, M.; Heyd, J. J.; Brothers, E.; Kudin,
477 K. N.; Staroverov, V. N.; Keith, T.; Kobayashi, R.; Normand, J.;
478 Raghavachari, K.; Rendell, A.; Burant, J. C.; Iyengar, S. S.; Tomasi, J.;
479 Cossi, M.; Rega, N.; Millam, J. M.; Klene, M.; Knox, J. E.; Cross, J. B.;
480 Bakken, V.; Adamo, C.; Jaramillo, J.; Gomperts, R.; Stratmann, R. E.;
481 Yazyev, O.; Austin, A. J.; Cammi, R.; Pomelli, C.; Ochterski, J. W.;
482 Martin, R. L.; Morokuma, K.; Zakrzewski, V. G.; Voth, G. A.; Salvador,
483 P.; Dannenberg, J. J.; Dapprich, S.; Daniels, A. D.; Farkas, O.;
484 Foresman, J. B.; Ortiz, J. V.; Cioslowski, J.; Fox, D. J. *Gaussian 09*,
485 revision B.01; Gaussian, Inc.: Wallingford, CT, 2010. 488